

Superfluid filaments of dipolar bosons in free space

Fabio Cinti,^{1,2,*} Alberto Cappellaro,^{3,†} Luca Salasnich,^{3,4,‡} and Tommaso Macrì^{5,§}

¹*National Institute for Theoretical Physics (NITheP), Stellenbosch 7600, South Africa*

²*Institute of Theoretical Physics, Stellenbosch University, Stellenbosch 7600, South Africa*

³*Dipartimento di Fisica e Astronomia Galileo Galilei and CNISM,
Università di Padova, via Marzolo 8, 35131 Padova, Italy*

⁴*CNR-INO, via Nello Carrara, 1 - 50019 Sesto Fiorentino, Italy*

⁵*Departamento de Física Teórica e Experimental, Universidade Federal do Rio Grande do Norte,
and International Institute of Physics, Natal-RN, Brazil*

(Dated: December 9, 2024)

We systematically investigate the zero temperature phase diagram of bosons interacting via dipolar interactions in three dimensions in free space via path integral Monte Carlo simulations based on the worm algorithm. Upon increasing the strength of the dipolar interaction and at sufficiently high densities we find a wide region where filaments are stabilized along the direction of the external field. Most interestingly by computing the superfluid fraction we conclude that superfluidity is anisotropic and vanishes along the orthogonal plane. Finally we perform simulations at finite temperature confirming the stability of filaments against thermal fluctuations and provide an estimate of the superfluid fraction in the weak coupling limit in the framework of the Landau two-fluid model. Such findings suggest that in the thermodynamic limit the system might crystallize into a regular array of superfluid filaments which are not globally phase coherent.

PACS numbers: 05.30.-d, 03.75.Hh, 03.75.Kk, 03.75.Nt, 67.85.De, 67.85.Bc, 67.80.K-

Superfluidity is an amazing phenomenon of quantum mechanical origin that manifests itself macroscopically as frictionless flow and lack of response to rotation for small enough angular velocity [1, 2]. Several experimental platforms have been used to investigate quantum matter in the superfluid regime [3]. Among them, ultracold gases realize a very clean and controllable many-body playground that permit the observation of quantum properties with unprecedented precision [4]. In these systems superfluidity has been observed both with bosonic as well as with fermionic atoms [5–8]. The superfluid fraction, the ratio of the superfluid density to the total density of the system, has been recently measured in two-component Fermi gas interacting via strong contact potentials [7, 9, 10].

An even richer phenomenology appears when long-range interactions are present. The non-local character of the interparticle potential may induce instabilities of the density that lead to a spontaneous breaking of translational symmetry. A primary example is the long sought supersolid state, where superfluidity is accompanied by a crystalline order [11–14]. Recent groundbreaking experiments with dipolar condensates demonstrated the existence of dense bosonic droplets in trapped configurations [15–18] and in free space [19]. Beyond mean-field effects [20–22] and three-body interactions [23] have been invoked as the main mechanisms responsible for the stability of these clusters. Large scale simulations based on a non-local non-linear Schrödinger equation have shown very good agreement with the density distribution and the excitation spectra observed in laboratory. Latest experiments paved the way for the search of phase coherence of droplets, demonstrating interference pattern via

expansion dynamics of the condensate. The presence of fringes showed that each droplet is individually phase coherent and thus superfluid, leaving yet unresolved the question of global phase coherence of the system [16].

In this Letter we report path-integral Monte Carlo (PIMC) results for the low temperature properties of a dipolar gas of bosons in three dimensional free space. Recent works showed with similar methods the existence of a window in parameter space leading to stable self-bound configurations of a single [24] or several droplets in a regular arrangement in trapped configurations [25]. Yet, no work has investigated the superfluid character of these structures. Here we address the issue of superfluidity of elongated filaments for a wide range of the strength of the dipolar interaction and density as well as their stability against finite temperature fluctuations. We carry out large scale simulations, based on a continuous-space worm algorithm which allows for an efficient and reliable determination of the superfluid density [26, 27]. We observe an anisotropic character of the superfluid fraction in the inhomogeneous regime of the filaments. Most importantly, we predict the absence of global phase coherence and therefore exclude the existence of supersolidity in three dimensional dipolar bosons.

The Hamiltonian of an ensemble of N interacting identical bosons is:

$$\hat{H} = - \sum_{i=1}^N \frac{\hbar^2}{2m} \nabla_i^2 + \sum_{i<j}^N V(\mathbf{r}_i - \mathbf{r}_j), \quad (1)$$

where m is the particle mass, \mathbf{r}_i is the position of the i -th dipole. We model the interparticle potential $V(\mathbf{r})$ by a short-range hard-core with cutoff r_0 and an anisotropic

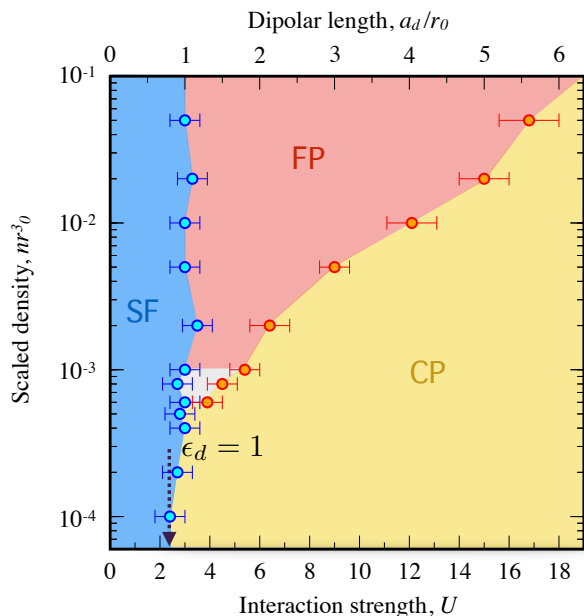


FIG. 1. Zero-temperature phases of dipolar bosons in three dimensions in free space: Superfluid (SF), superfluid filaments (FP) and non-superfluid cluster phases (CP) for varying dimensionless interaction strength U (or equivalently dipolar length a_d/r_0) and scaled density nr_0^3 . For $a_d/r_0 \lesssim 0.9$ the blue region labeled by SF corresponds to a uniform superfluid. For low densities the SF regime agrees with mean-field prediction that predicts stability for $a_d/a_s < 1$ (black dotted arrow at $a_d/r_0 = 0.75$). FP is encountered for high densities $nr_0^3 \gtrsim 5 \cdot 10^{-4}$ and for $a_d/r_0 \gtrsim 1$ and extends to strong couplings. For small densities $nr_0^3 \lesssim 5 \cdot 10^{-4}$ the system collapses directly into tiny clusters with vanishing superfluid fraction. The phase boundaries in the dashed region are not resolved.

long-range dipolar potential:

$$V(\mathbf{r}) = \begin{cases} \frac{C_{dd}}{4\pi} \frac{1-3\cos^2\theta}{r^3} & \text{if } r \geq r_0, \\ \infty & \text{if } r < r_0, \end{cases} \quad (2)$$

where $C_{dd}/4\pi$ is the coupling constant and the angle θ denotes the angle between the vector \mathbf{r} and the z -axis. Here the units of length and energy are r_0 and \hbar^2/mr_0^2 , respectively. Therefore the zero-temperature physics is controlled by the dimensionless interaction strength $U = mC_{dd}/4\pi\hbar^2r_0$ and the dimensionless density nr_0^3 only [28]. Eq.(1) applies both to vertically aligned dipoles interacting via magnetic or electric dipole moments [29]. The hard-core with radius r_0 removes the unphysical $1/r^3$ attraction of two aligned dipoles in head-to-tail configurations at small distances. Finite dipolar potentials affect the scattering length a_s associated to the contact potential into a non-trivial relation of C_{dd} [30–32]. This turns out to be crucial to account for the stability properties of a dipolar gas in generic (beyond) mean-field approaches. For example a standard Bogoliubov calculation determines the stability of a homogeneous condensate when $\epsilon_d \equiv a_d/a_s < 1$ is satisfied, where $a_d = \frac{C_{dd}m}{12\pi\hbar^2}$ is the

dipolar length associated to Eq.(2) [29, 33].

In order to assess systematically the zero temperature phases, we determine the equilibrium properties of Eq. (1) in a wide range of scaled average density nr_0^3 (different from experimentally measured peak density) and interaction strength U . We work in the canonical ensemble, i.e. fixing the particle number, chosen between $N = 100 - 400$ in a cubic box with linear dimension L with periodic boundary conditions. A strong decay of the dipolar potential with the distance precludes relevant effects of self-interaction. From these simulations we obtain, for example, density profiles, and pair correlation functions, as well as the superfluid fraction [34] at finite temperatures. The phases were obtained by extrapolating to the limit of zero temperature, lowering the temperature until observables, such as the total energy, superfluid fraction and pair correlations did not change on further decrease of T . These observables were then analyzed to construct the phase diagram in Fig.1 that we now discuss in detail. For clarity an additional horizontal axis displays the scaled dipolar length a_d/r_0 . In the weakly interacting regime the system is in a superfluid phase (SF) with unitary f_s . For low densities $nr_0^3 \lesssim 10^{-3}$ the SF extends up to $U \approx 2.25$ which agrees with the mean-field phase boundary predicted by standard Bogoliubov analysis ($\epsilon_d = 1$) for the dipolar potential and a contact interaction. Increasing the interaction strength the system enters into a cluster phase (CP) with vanishing superfluidity and characterized by droplet structures with few particles. For higher densities $nr_0^3 > 6 \cdot 10^{-4}$, crossing the SF phase boundary, we encounter a phase characterized by elongated filaments (FP) with anisotropic superfluid fraction (see below). We notice that this FP extends from small positive induced contact potential ($\epsilon_d \gtrsim 1$) which corresponds to the experimentally relevant regime of [15], to the strongly coupled limit of large dipolar interactions and large densities. For intermediate densities $6 \cdot 10^{-4} \lesssim nr_0^3 \lesssim 1 \cdot 10^{-3}$ the phase boundaries are not completely resolved (grey region in Fig.1).

Representative PIMC configurations with 100 particles and 500 imaginary-time slices ($nr_0^3 = 10^{-2}$) of the density distribution are shown in Fig.2. In the SF (Fig.2a) particles delocalize into a phase with uniform density displaying flat pair correlation functions, $g(r)$, typical of a fluid phase of particles interacting via hard-core potentials. In Fig.2b a typical configuration of the FP is illustrated where filaments elongate along the vertical direction. Finally in the CP several small clusters form, slightly elongated along the vertical direction, signaling a fragmentation of the filaments for large interactions. In the non-homogeneous FP and CP we analyze the pair correlation function $g(r)$ along two orthogonal directions. The function $g_{\parallel}(r)$ (red line in Fig.2) is computed along the vertical axis parallel to the direction of the filaments. In the FP $g_{\parallel}(r)$ has a liquid-like profile with a peak $r \gtrsim r_0$ as a consequence of the attractive part of the dipolar in-

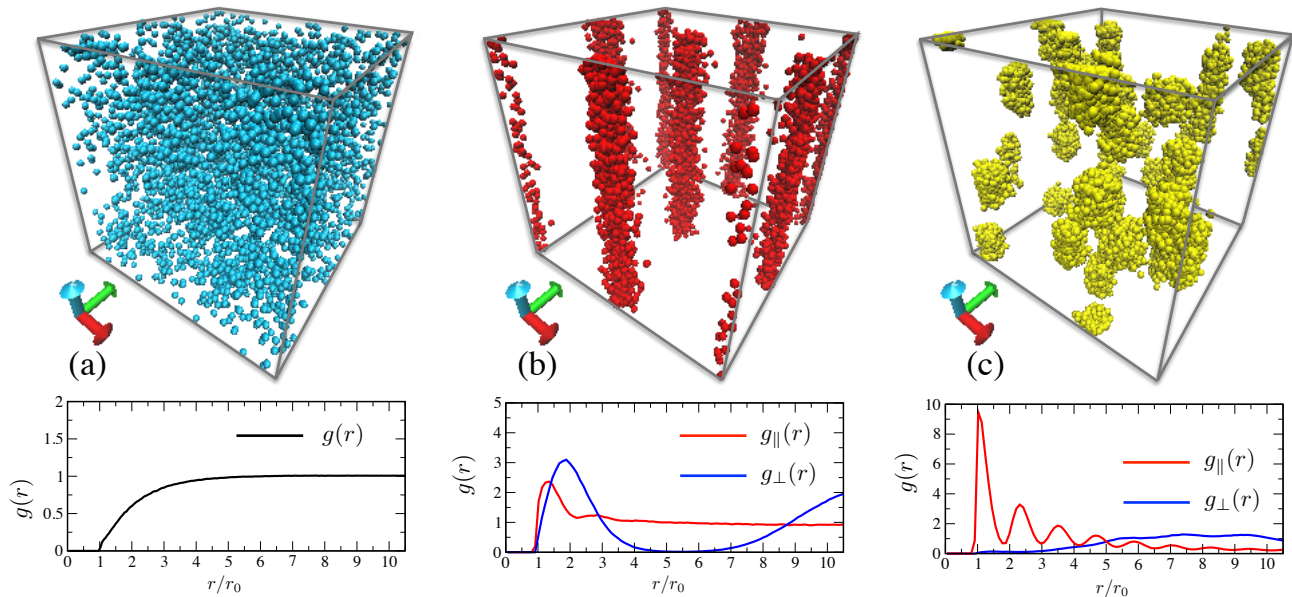


FIG. 2. Characterization of the phases at $nr_0^3 = 10^{-2}$. Upper panels. PIMC density distribution at different strengths of dipolar interaction: (a) SF at $a_d = 0.6r_0$, (b) superfluid FP at $a_d = 2.6r_0$ and (c) CP at $a_d = 6.0r_0$. Lower panels. (a) pair correlation functions $g(r)$ in the SF. (b) and (c) pair correlation functions $g_{\parallel}(r)$ along the vertical direction (red) and $g_{\perp}(r)$ along the orthogonal plane (blue). $g_{\parallel}(r)$ has a fluid-like profile in the FP. In the CP $g_{\parallel}(r)$ a high peak due to strong attractive interactions appears at distances $r \gtrsim r_0$. $g_{\perp}(r)$ in the FP shows a strong suppression in between two filaments whereas in the CP it flattens at intermediate distances. Simulations are done with 100 particles and 500 slices with periodic boundary conditions. Correlation functions are averaged over a hundred configurations.

interaction and the large density along the z -axis. In the CP the first peak of $g_{\parallel}(r)$ is higher and the function oscillates several times before vanishing for large distances as a consequence of the finite size of the clusters. The correlation $g_{\perp}(r)$ (blue line) is evaluated along the horizontal plane, perpendicular to the direction of the filaments. In the FP, it is strongly suppressed in the region between two filaments as expected from particle density distributions. In the CP $g_{\perp}(r)$ flattens at intermediate distances displaying an irregular arrangement of the small dipolar droplets along the horizontal plane.

To fully characterize the genuine quantum properties of the FP we compute the superfluid fraction $f_s^{(i)}$ as a function of the interaction strength and temperature along three orthogonal directions $i = x, y, z$, yielding $f_s^{(i)} = \frac{mk_B T}{\hbar^2 n} \langle w_i^2 \rangle$, where $\langle \dots \rangle$ stands for the thermal average of the winding number estimator w_i . [35, 36]. Fig.3 depicts the superfluid fraction $f_s^{(i)}$ calculated varying the dipolar length a_d for $nr_0^3 = 10^{-2}$. In the SF the superfluid density is uniform and unitary ($f_s^{(i)} = 1$). Crossing the SF-FP phase boundary $f_s^{(i)}$ displays a strong anisotropy. The superfluid fraction is unitary along the vertical direction and it vanishes along the orthogonal $x - y$ plane, showing only a marginal finite-size effect contribution to w_x and w_y , respectively. This result indicates that each filament is phase coherent, but globally the system is not. Finally entering in the CP $f_s^{(i)} = 0$

uniformly as expected from the fragmentation of the filaments in the configurations. The lower panel of Fig.3 reports the relative frequency of exchange cycles involving a particle number $1 \leq L \leq N$ [37]. In the SF we observe long permutation cycles ($\sim N$). In the FP (CP) cycles reduce to few tens of (few) particles in support of the previous observation that superfluidity originates within each filament (each cluster).

Finally we investigate the stability of superfluid filaments at finite temperatures. In Fig.4 we show the superfluid fraction for a system of $N = 100$ particles at density $nr_0^3 = 10^{-2}$ as a function of T/T_0 , T_0 being the critical temperature of an ideal Bose gas $k_B T_0 = \frac{2\pi}{\zeta(3/2)^{2/3}} (nr_0^3)^{2/3}$ [38]. We start by analyzing the superfluid fraction in the SF. We compare PIMC results with an analytical calculation within the Landau two-fluid model [39], which, for the SF, predicts the temperature dependence of the superfluid fraction as

$$f_s^{(z)} = 1 - \frac{\beta \hbar^2}{4\pi^2 m} \int_0^\infty dq \int_0^\pi d\theta_q q^4 \frac{\sin \theta_q \cos^2 \theta_q e^{\beta E_q}}{(e^{\beta E_q} - 1)^2} \quad (3)$$

where $E_{\mathbf{q}} = \sqrt{\frac{\hbar^2 q^2}{2m} \left(\frac{\hbar^2 q^2}{2m} + 2 \frac{\mu}{g_0} \tilde{V}_{\text{ps}}(\mathbf{q}) \right)}$ is the Bogoliubov spectrum. The function $\tilde{V}_{\text{ps}}(\mathbf{q}) = g_0 (1 - \epsilon_d + 3\epsilon_d \cos^2(\theta_q))$ is the Fourier transform of the pseudo-potential $V_{\text{ps}}(\mathbf{r}) = g_0 \delta(\mathbf{r}) + \frac{C_{dd}}{4\pi} \frac{1-3\cos^2 \theta}{r^3}$ with $g_0 = 4\pi \hbar^2 a_s / m$, which is widely used as a regularized

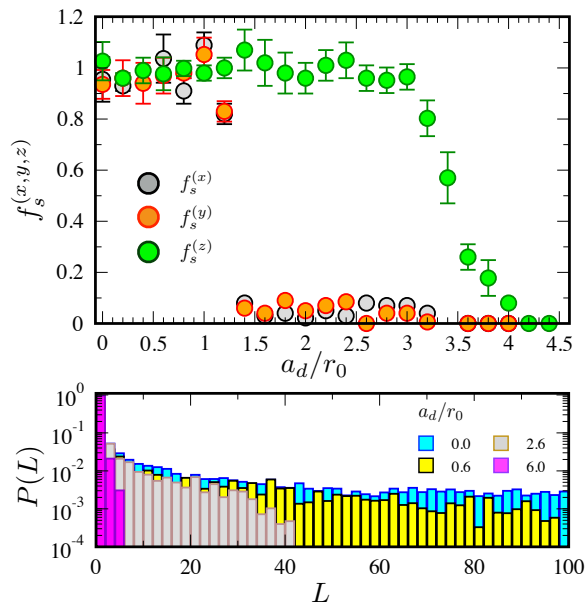


FIG. 3. Superfluid fraction f_s across the transition from superfluid to filament transition at high densities. Upper panel. f_s as a function of the dipolar length along the vertical direction and the orthogonal direction for $nr_0^3 = 10^{-2}$. Dipoles and filaments are aligned along the z -axis. In the SF the superfluid fraction converges to $f_s = 1$ isotropically. In the filaments we observe $f_s = 1$ along the vertical axis and vanishing on the orthogonal plane. Error bars are statistical uncertainties. Lower panel. Relative frequency of permutation cycles of length L again for $nr_0^3 = 10^{-2}$ and $a_d = 0, 0.6, 2.8, 6.0 r_0$ in the SF (blue and yellow), FP (grey) and CP (purple).

form of the interparticle potential (2) [29, 33, 40]. The chemical potential μ includes the beyond mean field contribution of the dipolar interaction:

$$\mu = g_0 n \left(1 + \frac{32}{3\sqrt{\pi}} \sqrt{na_s^3} Q_{5/2}(\epsilon_d) \right), \quad (4)$$

where $Q_\alpha(x) = \int_0^1 dt (1 - x + 3xt^2)^\alpha$ [41]. The plot of the superfluid fraction along the vertical axis from Eq.(3) is shown in Fig.4 for $a_d = 0$ (black line) and $a_d = 0.6 r_0$ (red dashed line). In the low temperature regime we can linearize $E_{\mathbf{q}}$ to determine an approximate analytical formula for the superfluid fraction:

$$\tilde{f}_s^{(z)} = 1 - \frac{2\pi^2}{45} \frac{1}{(1 - \epsilon_d)(1 + 2\epsilon_d)^{3/2}} \left(\frac{m}{\hbar^2} \right)^{3/2} \frac{(k_B T)^4}{n \mu^{5/2}}, \quad (5)$$

that works well up to $T \lesssim 0.3 T_0$. In the inset of Fig.4 we show the difference between the superfluid fractions of Eq.(3) and the analytical result Eq.(5) for the same values of a_d as in the main figure. For larger dipolar length $a_d = 2.6 r_0$, in the FP, the superfluid fraction along the vertical axis is finite within a large window of temperatures. We conclude then that filaments are stable against finite temperature fluctuations and we clearly see that

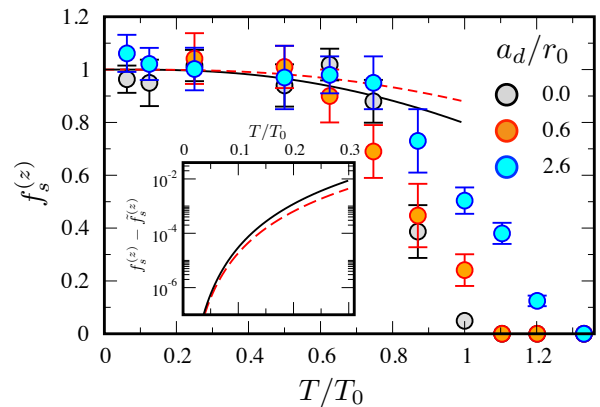


FIG. 4. Superfluid fraction $f_s^{(z)}$ as a function of the scaled temperature T/T_0 at $nr_0^3 = 10^{-2}$ for three values of the dipolar lengths: a) SF with $a_d = 0$ (hard-core bosons), b) SF with $a_d = 0.6 r_0$, c) FP with $a_d = 2.6 r_0$. Lines refer to the analytical prediction of the temperature dependence of the superfluid fraction at $nr_0^3 = 10^{-2}$ from Eq.(3) at $a_d = 0$ (black continuous line) and $a_d = 0.6 r_0$ (red dashed line). Inset. Low temperature limit of $f_s^{(z)}$ from Eq.(3) and Eq.(5) in the SF at $a_d = 0$ and $a_d = 0.6 r_0$.

anisotropic superfluidity is finite up to temperatures $T \sim 0.8 T_0$. We also verified that the orthogonal components of the superfluid fraction are vanishing in this regime.

Our results then suggest that the observed interference pattern [15] is a consequence of *local* phase coherence (within each filament) and not a *global* one (among the filaments). As discussed above the FP is characterized by an anisotropic superfluid density that, interestingly, might be measured via the second sound along the orthogonal directions as recently done with strongly interacting Fermi gases [5–8].

In this Letter we studied the many-body phases of an ensemble of bosons interacting via dipole-dipole interactions in three dimensional free space and investigated the superfluid behavior of dipolar filaments. We spanned a wide range of the parameter space confirming the existence of an extended phase of non-overlapping filaments with unitary superfluidity along the filaments and vanishing otherwise. Our results therefore theoretically support recent experimental findings about the stability of droplets in free space [19] and the presence of local phase coherence [15] giving rise to interference fringes but exclude global phase coherence of the filaments and therefore a possible supersolid phase in the thermodynamic limit. Finally we confirmed that such a filament phase is stable at finite temperature. More refined investigations are needed to determine accurately the melting transition of the filaments into a fluid phase.

Acknowledgments. We thank R. N. Bisset, M. Boninsegni, S. Giorgini, G. Gori, A. Pelster, T. Pohl, G. Shlyapnikov, F. Toigo and M. Troyer for useful discussions and I. Ferrier-Barbut for helpful correspondence.

T.M. acknowledges CNPq for support through Bolsa de produtividade em Pesquisa n. 311079/2015-6 and thanks NITheP for the hospitality where part of the work was done. F.C. acknowledges the hospitality of the MPI-PKS in Dresden where part of the work was carried out.

* cinti@sun.ac.za

† cappellaro@pd.infn.it

‡ luca.salasnich@unipd.it

§ macri@fisica.ufrn.br

- [1] L. Pitaevskii and S. Stringari, *Bose-Einstein Condensation* (Oxford University Press, USA, 2003).
- [2] C. Pethick and H. Smith, *Bose-Einstein condensation in dilute gases* (Cambridge University Press, Cambridge, England, 2002).
- [3] A. J. Leggett, *Quantum liquids Bose condensation and Cooper pairing in condensed-matter systems* (Oxford University Press, 2006).
- [4] I. Bloch, J. Dalibard, and W. Zwerger, *Rev. Mod. Phys.* **80**, 885 (2008).
- [5] L. Verney, L. Pitaevskii, and S. Stringari, *EPL (Europhysics Letters)* **111**, 40005 (2015).
- [6] M. K. Tey, L. A. Sidorenkov, E. R. S. Guajardo, R. Grimm, M. J. H. Ku, M. W. Zwierlein, Y.-H. Hou, L. Pitaevskii, and S. Stringari, *Phys. Rev. Lett.* **110**, 055303 (2013).
- [7] L. P. Pitaevskii and S. Stringari, (2015), arXiv:1510.01306.
- [8] Y.-H. Hou, L. P. Pitaevskii, and S. Stringari, *Phys. Rev. A* **88**, 043630 (2013).
- [9] L. Salasnich, *Phys. Rev. A* **82**, 063619 (2010).
- [10] L. A. Sidorenkov, M. K. Tey, R. Grimm, Y.-H. Hou, L. Pitaevskii, and S. Stringari, *Nature* **498**, 78 (2013).
- [11] M. Boninsegni and N. V. Prokof'ev, *Rev. Mod. Phys.* **84**, 759 (2012).
- [12] F. Cinti, T. Macri, W. Lechner, G. Pupillo, and T. Pohl, *Nature Communications* **5**, 3235 EP (2014).
- [13] J. Léonard, A. Morales, P. Zupancic, T. Esslinger, and T. Donner, (2016), arXiv:1609.09053.
- [14] J. Li, J. Lee, W. Huang, S. Burchesky, B. Shteynas, F. Ç. Top, A. O. Jamison, and W. Ketterle, (2016), 1610.08194.
- [15] H. Kadau, M. Schmitt, M. Wenzel, C. Wink, T. Maier, I. Ferrier-Barbut, and T. Pfau, *Nature* **530**, 194 (2016).
- [16] I. Ferrier-Barbut, H. Kadau, M. Schmitt, M. Wenzel, and T. Pfau, *Phys. Rev. Lett.* **116**, 215301 (2016).
- [17] L. Chomaz, S. Baier, D. Petter, M. J. Mark, F. Wächtler, L. Santos, and F. Ferlaino, *Phys. Rev. X* **6**, 041039 (2016).
- [18] I. Ferrier-Barbut, M. Schmitt, M. Wenzel, H. Kadau, and T. Pfau, *Journal of Physics B: Atomic, Molecular and Optical Physics* **49**, 214004 (2016).
- [19] M. Schmitt, M. Wenzel, F. Böttcher, I. Ferrier-Barbut, and T. Pfau, *Nature* **539**, 259 (2016).
- [20] F. Wächtler and L. Santos, *Phys. Rev. A* **93**, 061603 (2016).
- [21] R. N. Bisset, R. M. Wilson, D. Baillie, and P. B. Blakie, *Phys. Rev. A* **94**, 033619 (2016).
- [22] D. Baillie, R. M. Wilson, R. N. Bisset, and P. B. Blakie, *Phys. Rev. A* **94**, 021602 (2016).
- [23] R. N. Bisset and P. B. Blakie, *Phys. Rev. A* **92**, 061603 (2015).
- [24] H. Saito, *Journal of the Physical Society of Japan* **85**, 053001 (2016).
- [25] A. Macia, J. Sánchez-Baena, J. Boronat, and F. Mazzanti, *Phys. Rev. Lett.* **117**, 205301 (2016).
- [26] M. Boninsegni, N. Prokof'ev, and B. Svistunov, *Phys. Rev. Lett.* **96**, 070601 (2006).
- [27] M. Boninsegni, N. V. Prokof'ev, and B. V. Svistunov, *Phys. Rev. E* **74**, 036701 (2006).
- [28] The scaled density nr_0^3 coincides with the usual definition of the gas parameter na_s^3 in the limit of vanishing dipolar interaction, that is $C_{dd} \rightarrow 0$. See also below and [30, 31].
- [29] T. Lahaye, C. Menotti, L. Santos, M. Lewenstein, and T. Pfau, *Reports on Progress in Physics* **72**, 126401 (2009).
- [30] D. C. E. Bortolotti, S. Ronen, J. L. Bohn, and D. Blume, *Phys. Rev. Lett.* **97**, 160402 (2006).
- [31] S. Ronen, D. C. E. Bortolotti, D. Blume, and J. L. Bohn, *Phys. Rev. A* **74**, 033611 (2006).
- [32] R. Oldziejewski and K. Jachymski, *Phys. Rev. A* **94**, 063638 (2016).
- [33] M. A. Baranov, M. Dalmonte, G. Pupillo, and P. Zoller, *Chemical Reviews* **112**, 5012 (2012).
- [34] B. Svistunov, E. Babaev, and N. Prokof'ev, *Superfluid States of Matter* (Taylor & Francis, 2015).
- [35] E. L. Pollock and D. M. Ceperley, *Phys. Rev. B* **36**, 8343 (1987).
- [36] D. M. Ceperley, *Rev. Mod. Phys.* **67**, 279 (1995).
- [37] P. Jain, F. Cinti, and M. Boninsegni, *Phys. Rev. B* **84**, 014534 (2011).
- [38] An extensive calculation of the critical temperature with of dipolar interactions is not reported here. Indeed it can be done along the lines of [42] and it is the focus of a separated investigation.
- [39] M. Ghabour and A. Pelster, *Phys. Rev. A* **90**, 063636 (2014).
- [40] M. A. Baranov, *Physics Reports* **464**, 71 (2008).
- [41] A. R. P. Lima and A. Pelster, *Phys. Rev. A* **84**, 041604 (2011).
- [42] S. Pilati, S. Giorgini, and N. Prokof'ev, *Phys. Rev. Lett.* **100**, 140405 (2008).